This study investigates a capsule-type SGK 538/160–70M hydrogenerator with a rated power of 23 MVA. The task addressed relates to crack initiation and failure of the damper winding in the hydrogenerator in the presence of rotor static eccentricity.

A three-dimensional field-based mathematical model of the electromagnetic–thermal–mechanical interaction has been constructed to evaluate the distributions of currents, temperatures, and thermomechanical stresses in the damper winding segment and in the brazed joints of rods.

It is shown that the occurrence and evolution of rotor static eccentricity constitute one of the essential causes of catastrophic damages and failures in hydrogenerators of this type. It has been determined that, under rotor static eccentricity of $\varepsilon = 0.83$, the local stresses in the joint of the central rod increase by a factor of ~3.2 (up to ≈ 540 MPa). This value exceeds the tensile strength of copper and explains rod ruptures and avalanche-type failure of the segment. In addition, it was established that the existence and localization of cracks in brazed joints significantly affect the bending (deformation) behavior of the pole damper winding segment.

The results could be applied to estimate the service life and to upgrade large slow-speed synchronous hydrogenerators (including capsule types). Specifically, under the following conditions:

a) existing or expected eccentricities;

b) high thermal gradients in the end/short-circuiting parts of the damper winding;

c) operation with frequent starts/stops or cooling modes close to limiting values.

The effective engineering measures that have been proposed, such as improving the mobility of rods in slots; revising the number and diameters of rods; applying high-strength materials, could be implemented in retrofitting projects and when repairing the rotor

Keywords: capsule hydrogenerator, rotor eccentricity, rods damage, damper winding, thermomechanical stresses

UDC 621.313
DOI: 10.15587/1729-4061.2025.342108

IDENTIFYING MECHANISMS BEHIND CRACK FORMATION AND DESTRUCTION OF THE DAMPER WINDING OF A CAPSULE-TYPE HYDROGENERATOR IN THE PRESENCE OF STATIC ROTOR ECCENTRICITY

Olexandr Geraskin
Corresponding author
PhD, Associate Professor*
E-mail: fegasusr@gmail.com
Yurii Haidenko
PhD, Associate Professor*
Vadim Chumack
PhD, Professor*
Vladislav Mihaylenko
PhD, Associate Professor**
Yevhenii Trotsenko
PhD, Associate Professor**
*Department of Electromechanics***
Department of Theoretical Electrical Engineering*
***National Technical University of Ukraine
«Igor Sikorsky Kyiv Polytechnic Institute»
Beresteiskyi ave., 37, Kyiv, Ukraine, 03056

Received 05.08.2025
Received in revised form 01.10.2025
Accepted 17.10.2025
Published 31.10.2025

How to Cite: *Geraskin, O., Haidenko, Y., Chumack, V., Mihaylenko, V., Trotsenko, Y. (2025). Identifying mechanisms behind crack formation and destruction of the damper winding of a capsule-type hydrogenerator in the presence of static rotor eccentricity. Eastern-European Journal of Enterprise Technologies, 5 (7 (137)), 28–39. https://doi.org/10.15587/1729-4061.2025.342108*

1. Introduction

Ensuring the stability of electricity generation and the reliability of local and combined power systems is largely determined by the reliable operation of hydrogenerators (HGs). An important advantage of such units is their ability to quickly change operating modes, providing maneuverable power and primary/secondary regulation. During HG operation, it is important to maintain optimal load modes, monitor the technical condition of the nodes, and carry out preventive measures in a timely manner. At the same time, even with proven technologies, long-term operation of the equipment is accompanied by wear, the appearance of defects, and a decrease in efficiency, which results in a range of reliability issues. Against this background, the task of identifying critical damage mechanisms and their quantitative assessment arises.

High-power synchronous HGs are vulnerable to static/dynamic eccentricity defects and the associated unbalanced magnetic attraction, which provoke overvoltage and damage to the damper winding (DW) [1, 2]. Capsule designs (such as Straflo) are particularly sensitive to such defects due to the small air gap, significant axial and radial stress gradients, difficult heat dissipation, and increased cyclic loading on the solder joints. It is obvious that a reliable quantitative assessment of currents, temperatures, and thermomechanical stresses in the damper winding in the presence of static eccentricity requires three-dimensional coupled electromag-

netic-thermal-mechanical modeling. Such models should be able to localize the crack initiation zone in the solder joints and segments and explain the mechanisms of their subsequent failure.

A structural feature of the capsule type SGK 538/160–70M HG (used at the Kyiv and Kaniv HPPs of the Dnieper cascade) is a very small air gap (6 mm) with a large rotor diameter (4.918 m), which creates prerequisites for the emergence of rotor eccentricity. Static eccentricity (SE) of the rotor is more characteristic of HG of this type and may even lead to friction of the rotor against the stator core, which immediately requires the HG to be removed for repair. Smaller levels of SE lead to significant TMD and DW damage. In view of this, it is obvious that ensuring reliable operation of capsule hydrogenerators in the presence of static eccentricity is an urgent scientific and technical task. In-depth study of electromagnetic processes in damper systems with such deviations is important for preventing emergency modes and increasing the durability of equipment. The results could lay the foundation for improving methods for diagnosing and maintaining high-power HGs.

2. Literature review and problem statement

The task of investigating heating and mechanical stresses in the structural elements of HG is addressed in [3–12]. In general, the literature demonstrates that static/dynamic eccentricity, non-uniform electromagnetic fields, and cooling features significantly affect the distributions of currents, temperatures, and thermomechanical stresses (TMSs) in the DW and pole elements.

In work [3], the physical processes in the damper system of the rotor of a six-pole synchronous machine with a capacity of 500 kW, which cause the gradual destruction of its structure, were investigated. In particular, the distributions of currents, temperatures, and thermomechanical stresses in the damper winding rods during generator operation under asynchronous and asymmetric modes, as well as when rotor eccentricity occurs, were investigated. A two-dimensional field mathematical model has been built that takes into account the joint action of three physical fields of different nature, electromagnetic, temperature, and thermomechanical stress fields, and makes it possible to estimate heating and thermomechanical loads in the damping system of the rotor of a salient-pole synchronous machine. The limitation of the approach is the 2D formulation, due to which mainly point, rather than full-field (3D) TMS modeling results are reported.

In [4], the distributions of induced currents, temperatures, and thermomechanical stresses in the rotor damping winding rods of a capsule hydrogenerator of the SGK 538/160-70M type were investigated using mathematical modeling methods in the presence of a typical defect – the emergence of static rotor eccentricity. It is shown that in the presence of significant rotor eccentricity, large and significantly unevenly distributed currents are induced in the rotor rods. They, in turn, cause uneven heating and asymmetric TMS, which are dangerous and lead to rapid destruction of rotor's DW. At the same time, the 2D formulation and simplified analytical model of the pole limit the evaluation of spatial gradients and local extrema of TMS. This is a significant drawback of paper [4].

In [5], the three-dimensional distribution of TMS in the rotor core rods of the SGK 538/160–70M capsule hydrogenerator type was studied using mathematical modeling methods in the presence of a characteristic defect – the static eccentricity of the rotor. It was shown that at large values of eccentricity, significantly uneven TMSs appear in the rods, the values of which are dangerous and contribute to the rapid destruction of rotor DW. The disadvantage of the work is a limited overview of the problem and the lack of analysis of the nucleation/localization of cracks in joints (solder joints) and segments.

Taking into account the practice of [3–5], it is obvious that it is advisable to build and apply coupled 3D models of electromagnetic, thermal, and mechanical analysis, which make it possible to localize TMS peaks in critical zones – rod solder joints and short-circuiting segments.

In [6], damage on the pole shoe surface of a powerful capsule hydrogenerator is investigated, both based on real damage characteristics and in combination with physical field analysis. Failure mechanisms are shown with respect to operating conditions, design, and materials; troubleshooting methods and design improvement strategies are proposed. At the same time, the spatial distributions of mechanical stresses in the rotor pole elements remain incompletely investigated as the emphasis is on temperature observations.

In [7], a 3D model of air flow distribution and temperature field was constructed for a 1000 MW hydrogenerator under development based on the design of a 250 MW fanless air-cooled hydrogenerator. Using the computational flow dynamics approach, the cooling air flow distribution and temperature distribution in the rotor structure were investigated. Most attention was paid to axial and radial changes in the directions of cooling air flows between adjacent poles. In addition, a detailed study of the patterns of changes in the heat transfer coefficients of pole shoes and damper rods was carried out. The calculated temperature of the excitation windings coincided with the measured value.

In [8], the electromagnetic field of a 250 MW hydrogenerator was calculated and the power losses and heating in the rotor elements were determined; the influence of structural elements on the distribution of cooling air and temperature was analyzed using the finite volume method. The results were compared with the experiment.

Despite the thermal models built in [7, 8], the methodological basis for the direct determination of TMSs in structural elements remains insufficient. Further research is required to integrate thermal models with strength calculations for the correct assessment of local stresses.

In [9], the authors analyzed the waveforms of the no-load voltage, losses in the damper rods, and heat release when varying the rod pitch and the bevel of the stator slots in a 36 MW capsule hydrogenerator. Field electromagnetic models were constructed taking into account electrical circuits and a 3D thermal model of the rotor. It was found that a rational increase in the rod pitch and the bevel of the slots improve the voltage shape and reduce the temperature of the rods. However, the influence of these parameters on TMSs in pole elements and the relationship with potential damage was considered to a limited extent.

In study [10], the authors constructed models for analyzing the electromagnetic field, power losses in the DW

and heat generation in a capsule hydrogenerator with a capacity of 36 MW. The results showed that the electromagnetic field model for the steady-state mode does not fully take into account several key factors, such as tooth and groove effects, the main magnetic field, and the armature reaction. At the same time, it is more effective compared to the electromagnetic field model with step integration under the transient mode. As a result, the magnetic field, losses in the damper rods, and heat generation calculated by this model have significant deviations from observations on a real generator. In comparison, the electromagnetic field model with step integration under the transient mode of motion, due to the ability to take these factors into account, provides more comprehensive and justified results. However, mechanical stresses and damage to pole elements were not investigated in [10] – the focus was on comparing electromagnetic field models.

In [11], variants of capsule hydrogenerator designs with an integer and fractional number of slots per pole and phase were considered. Trends in the influence of different degrees of slot offset on the quality of the no-load voltage waveforms, losses in the DW and heat dissipation in the rated load mode were found. These results were also compared with data for the classical hydrogenerator design with a stator beveled by one slot. It is shown that for a generator with an integer number of slots, the offset scheme provides a voltage shape close to the classical scheme with a stator beveled by one slot – with lower losses/heat dissipation in DW. And for fractional numbers of slots, the results are opposite. The issues of the influence of uneven heating of rods on TMSs in short-circuited segments and the initiation of damage remained outside the scope of the analysis.

In [12], the authors analyzed the main causes of damage to the damper rods on the leeward side of the rotor poles and proposed a way to optimize the design of a 24 MW hydrogenerator. The distributions of eddy current densities in the damper rods were investigated and the phenomenon of their asymmetric distribution over the rod area was revealed. Based on the study of the distribution of eddy currents under various conditions, it was confirmed that the main factors affecting the asymmetric distribution of eddy currents in the damper rods are the stator slots and the armature reaction. However, in-depth modeling of mechanical stresses and mechanisms of damage formation in the DW was not performed since the emphasis was on electromagnetic aspects.

Despite significant progress in the study of electromagnetic and thermal processes in HGs, the complex influence of SE on thermomechanical phenomena in DW remains insufficiently studied. Available papers are mostly limited to simplified formulations or do not take into account the initiation and evolution of cracks in critical zones, which makes it impossible to reliably predict failures. Thus, the task to establish the mechanisms of damage and loss of integrity of the damper winding under conditions of spatial non-uniformity of fields and structural defects remains to be solved.

3. The aim and objectives of the study

The purpose of our study is to identify mechanisms behind the processes of crack formation and destruction of the damper winding of a capsule-type hydrogenerator in the presence of static eccentricity of the rotor. This will make it possible to identify the weakest points of DW from a mechanical point of view and subsequently improve the DW structure.

To achieve this aim, the following objectives were accomplished:

– to determine the sites of possible occurrence of DW cracks;

– to simulate the emergence of cracks near the extreme and central rods of DW;

– to simulate the emergence of a crack in the middle of the outer surface of the short-circuit segment;

– to simulate the separation of the central rod of DW;

– to simulate the free bending deformations of the short-circuit segment of DW.

4. The study materials and methods

The object of our study was the SGK 538/160–70M type capsule hydrogenerator with the following specifications: linear voltage of the stator winding – 6.3 kV; stator winding current – 2,070 A; power factor (shift) cosφ – 0.974; efficiency – 96.1%. It is also known that the number of poles is 70; the length of the active part of the rotor is 1.6 m; one-sided air gap under the middle of the pole $\delta = 6$ mm. Mechanical parameters of the copper of the DW rotor rods: the yield strength is $\sigma_{tk\_Cu} = 280$ MPa, and the strength limit is $\sigma_{mc\_Cu} = 390$ MPa. On each pole of the rotor there are three copper DW rods with a diameter of 17.5 mm and a length of 1.653 m, which are soldered to the short-circuiting segments. The soldering point is often termed a "solder joint" in the literature. Parts of DW at different poles are electrically connected by jumpers (longitudinal-transverse type of DW design).

The hypothesis of the study assumes that the SE of the rotor of the capsule HG is a determining factor in the origin and evolution of DW damage since it causes spatial non-uniformity of electromagnetic, thermal, and thermomechanical fields, which is critical for maintaining its structural integrity.

The following assumptions were adopted regarding the geometry of defects:

1. To determine potential crack formation zones, preliminary modeling of TMSs was performed for the intact DW; critical areas were identified: solder joints of the extreme and central rods and the middle of the outer surface of the short-circuiting segment.

2. The crack shape was assumed to be wedge-shaped for the entire thickness of the solder joint (up to 2 mm) adjacent to the short-circuiting segment; the wedge angle was 2°.

3. Cracks were modeled in the solder joints of two rods – the extreme (left) and central rod.

4. A crack of similar size was modeled in the middle of the solid outer surface of the short-circuiting segment of DW.

The following simplifications were accepted in the study:

1. Calculations are performed for a pole located near the minimum air gap that arose as a result of SE.

2. The simulation was carried out for the steady-state mode of HG at the rated symmetrical load.

3. Only the following rotor faults were considered: significant rotor SE with a value of $\varepsilon = 0.83$ (displacement ≈ 5 mm) and the presence of cracks in the rod solder joints and in the short-circuiting segment of DW.

The simulation of electromagnetic, thermal, and mechanical processes was performed in the COMSOL Multiphysics environment using the AC/to, Heat Transfer in Solids, and Structural Mechanics modules. To reproduce the real interaction of fields, a sequential multiphysics coupling was applied: electromagnetic problem → thermal problem → strength problem.

At the stage of calculating electromagnetic fields, a three-dimensional distribution of current density in the rods and short-circuited segments of DW was determined. Joule losses are automatically transferred to the thermal model as volumetric heat sources, which ensures the consistency of physical fields and realistic heating distribution.

The thermal model determines the spatial temperature field, which is used as a thermal load for estimating mechanical deformations and equivalent stresses at the next stage. This approach makes it possible to reproduce local stress concentrators in the areas of welds and potential cracks.

To correctly reproduce electrical processes, an equivalent electrical circuit of DW was constructed. Each rod is modeled by a branch with the corresponding resistance and inductance parameters, short-circuiting segments are modeled by similar elements, and interpole jumpers take into account their own electrical characteristics. This scheme makes it possible to take into account local effects of SE, correctly reproduce the distribution of currents in the pole, and transfer Joule losses to the thermal model for a realistic assessment of the heating of joints and segments.

The boundary conditions of heat exchange take into account the capsule design of the rotor and local axial and radial velocity gradients of the cooling medium. The thermal conductivity of materials and contact heat exchange in the weld zones were determined according to reference and specifications data. Test calculations were carried out to assess the sensitivity of the results to variations in convection coefficients and the stability of the computational process.

The basic output indicators are the spatial distributions of current density, temperature, and equivalent mechanical stresses. Special attention was paid to local stress maxima in the weld zones and short-circuiting segments since these areas are potentially dangerous for the integrity of the winding. Additionally, the influence of the localization and orientation of nucleated cracks on the deformation shape of the short-circuiting segments was analyzed. The computational process was implemented using a segregated solver, which makes it possible to control the convergence of the mesh, especially in areas with stress concentration. The correctness of the model was verified by comparing the energy balance of the electromagnetic and thermal problems, analyzing the mesh convergence in critical zones, and assessing the sensitivity of the results to changes in the cooling boundary conditions. This approach provides a comprehensive assessment of the relationship between electromagnetic, thermal, and thermomechanical processes, which is critically important for predicting the emergence of cracks and the DW failure in a capsule HG.

5. Results of research into the processes of crack formation and fracture of the damper winding of a rotor with eccentricity

5. 1. Determining the sites of possible occurrence of cracks in the damper winding based on a mathematical model

The mathematical model takes into account the interaction of three physical processes: electromagnetic, thermal, and thermomechanical (taking into account both heating and centrifugal mechanical stresses at rotor rotation). According to the results of our calculations, the currents in the rods and short-circuit segments of DW, which arise when SE appears, were determined. These currents are the primary source of DW heating.

Thermal power losses in the rods and short-circuit segments of DW are determined from the following formula

$$Q(x,y,z) = \left|J(x,y,z)\right|^2 \Big/ \gamma, \tag{1}$$

where γ is the electrical conductivity of DW material, J is the current density.

The mathematical model of the temperature field is based on the stationary differential equation of heat conduction. In Cartesian coordinates in the three-dimensional statement, the equation is written as follows

$$\lambda\left[\frac{\partial^2\theta(x,y,z)}{\partial x^2}+\frac{\partial^2\theta(x,y,z)}{\partial y^2}+\frac{\partial^2\theta(x,y,z)}{\partial z^2}\right]= -Q(x,y,z), \tag{2}$$

where $\theta(x, y, z)$ is the unknown temperature distribution function; λ is the thermal conductivity coefficient; $Q(x, y, z)$ is the volumetric specific sources of the thermal field [W/m^3], which, in fact, are Joule losses in DW.

The field three-dimensional mathematical model of the stress-strain state of DW within one pole is based on a system of partial differential equations of stationary problems in structural mechanics. In general, this system of equations takes the following form

$$\begin{cases} 0 = \nabla \cdot F \cdot S + \vec{F}, \\ F = \nabla u + I, \end{cases} \tag{3}$$

where ∇ – Hamilton operator; S – force tensor; F – strain gradient tensor; ∇u – displacement gradient; I – moment of inertia; $\vec{F}$ – distributed mass force vector (temperature strain force).

The basic calculated quantity for analyzing the stress-strain state is the von Mises mechanical stress tensor. It characterizes the average value of mechanical stresses that arise in a unit volume of material under the influence of the joint action of force factors of different spatial directions and different physical nature.

Experience in the operation of the studied HG has shown that damage to the pole DW often occurs at the end of its segment (Fig. 1, *a*). However, there is a need for a more in-depth study of the sites of possible emergence of cracks in the damper winding using mathematical modeling methods. Fig. 1, *a* shows the detachment of the short-circuited segment of the damper winding, the burnout of steel around the pole rods in the studied HG [4].

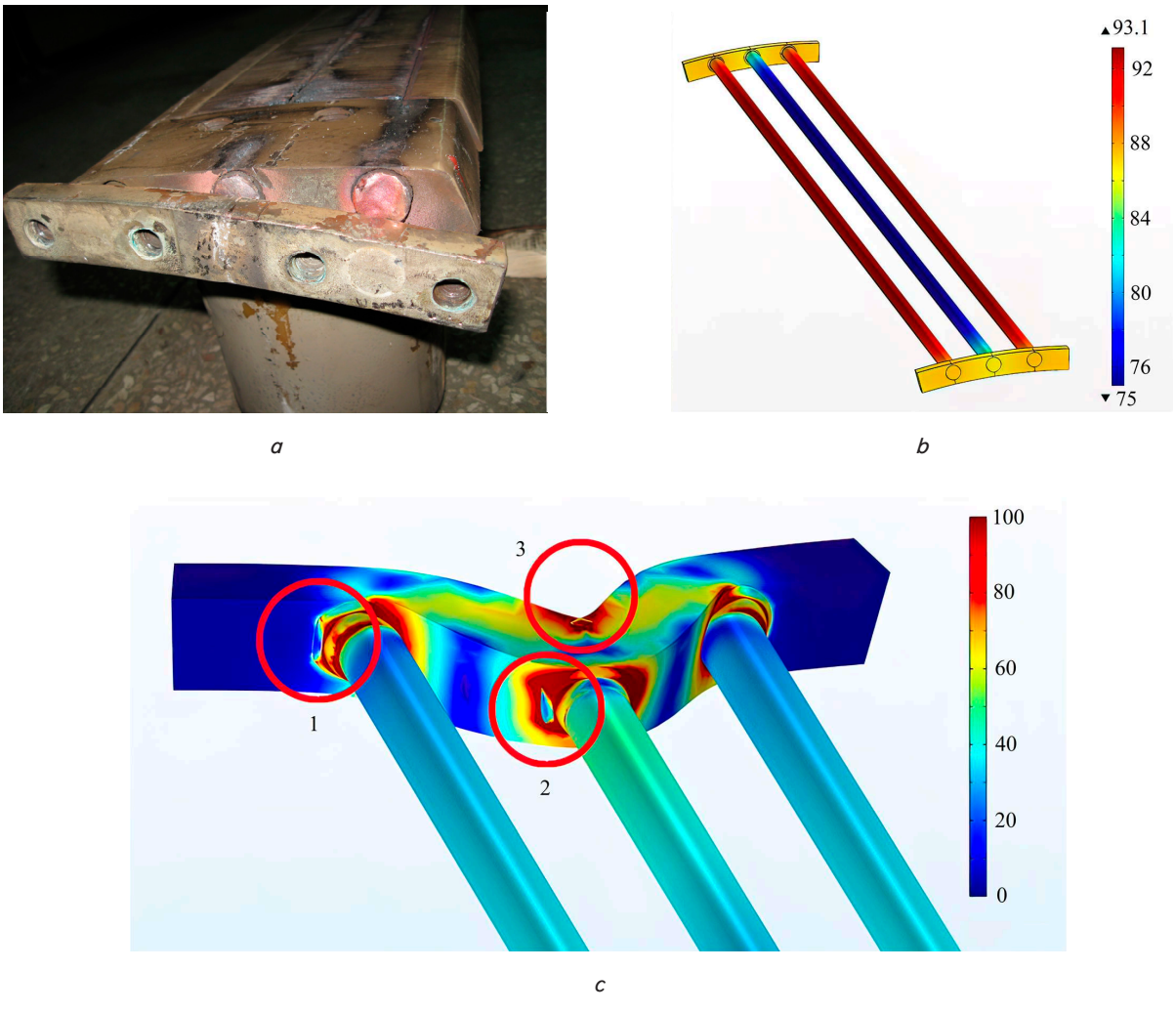

Fig. 1. The studied SGK 538/160–70M type hydrogenerator: *a* – photograph of a pole with a torn off short-circuiting segment of the damper winding and steel burnout around the rods; *b* – temperature distributions in the damper winding of one pole (°C) obtained from the simulation results; *c* – thermomechanical stresses in the damper winding at a static rotor eccentricity $\varepsilon = 0.83$ (MPa, deformation values are increased 500 times for clarity)

The process of modeling the heating of DW was carried out on the basis of the results from calculating its electrical circuit, which is given in [4]. At the same time, the currents in it were distributed in a certain way in accordance with the studied level of SE. The results of modeling the heating of the DW fragment within one pole in the presence of rotor SE (and without cracks) are shown in Fig. 1, *b*.

Fig. 1, *c* shows the distribution of TMSs in the volume of the short-circuit segment and DW rods in the presence of rotor SE with a value of $\varepsilon = 0.83$, in particular, red colors correspond to larger values of TMS values. For a better demonstration of the spatial shape of the bending of the DW fragment, the values of thermomechanical deformations were intentionally increased by 500 times.

In Fig. 1, *c*, the three most loaded areas, from the point of view of TMSs, are clearly visible:

– area 1 – in the extreme rods from the end side of the short-circuiting segment (mark 1 in Fig. 1, *c*). In this zone, a crack can potentially appear in the solder joint between the rod and the short-circuiting segment;

– area 2 – between the central rod and the short-circuiting segment (mark 2 in Fig. 1, *c*). Similarly to Area 1, such a deflection can cause a crack in the solder joint between the rod and the short-circuiting segment, or even a rod detachment;

– area 3 – in the middle of the outer surface of the short-circuiting segment (mark 3 in Fig. 1, *c*). In this zone, a potential crack can form due to alternating forces acting on the short-circuiting segment in the presence of SE: periodic transition of HG from the operating mode to the idle mode and vice versa.

5. 2. Modeling of cracks near the extreme and central rods of the damper winding

In order to determine the maximum values of TMSs that occur in the depth of the solder joints, the results of modeling the above segment of DW (Fig. 1, *c*) were analyzed in more detail. For this purpose, the values and distribution of TMSs were determined in the axial section (two-dimensional plane) of the DW segment (Fig. 2, *a*). The scale on the right is conditionally limited to 50 MPa so that the TMS distribution in the figure is more pronounced. In the upper part of Fig. 2, *a*, red circles outline the areas of the solder joints in which there are cracks. At the same time, the lower part of Fig. 2, *a* reflects a variant of an intact DW (without cracks) but with the existing SE of the HG rotor.

From the lower part of Fig. 2, *a* it is clear that in the solder joints there are small values of TMSs. Thus, from the outside around the extreme rods (where the tensile forces act) TMS is 62 MPa. And from the inside of the extreme rods (where the compressive forces act) TMS is 159 MPa. Around the central rod, TMS is 167 MPa. When cracks appear (upper part of Fig. 2, *a*), these TMS values will increase sharply.

Fig. 2, *b*–*d* shows (magnified) areas around the solder joint of the extreme and central rods both in the absence of a crack and when it appears.

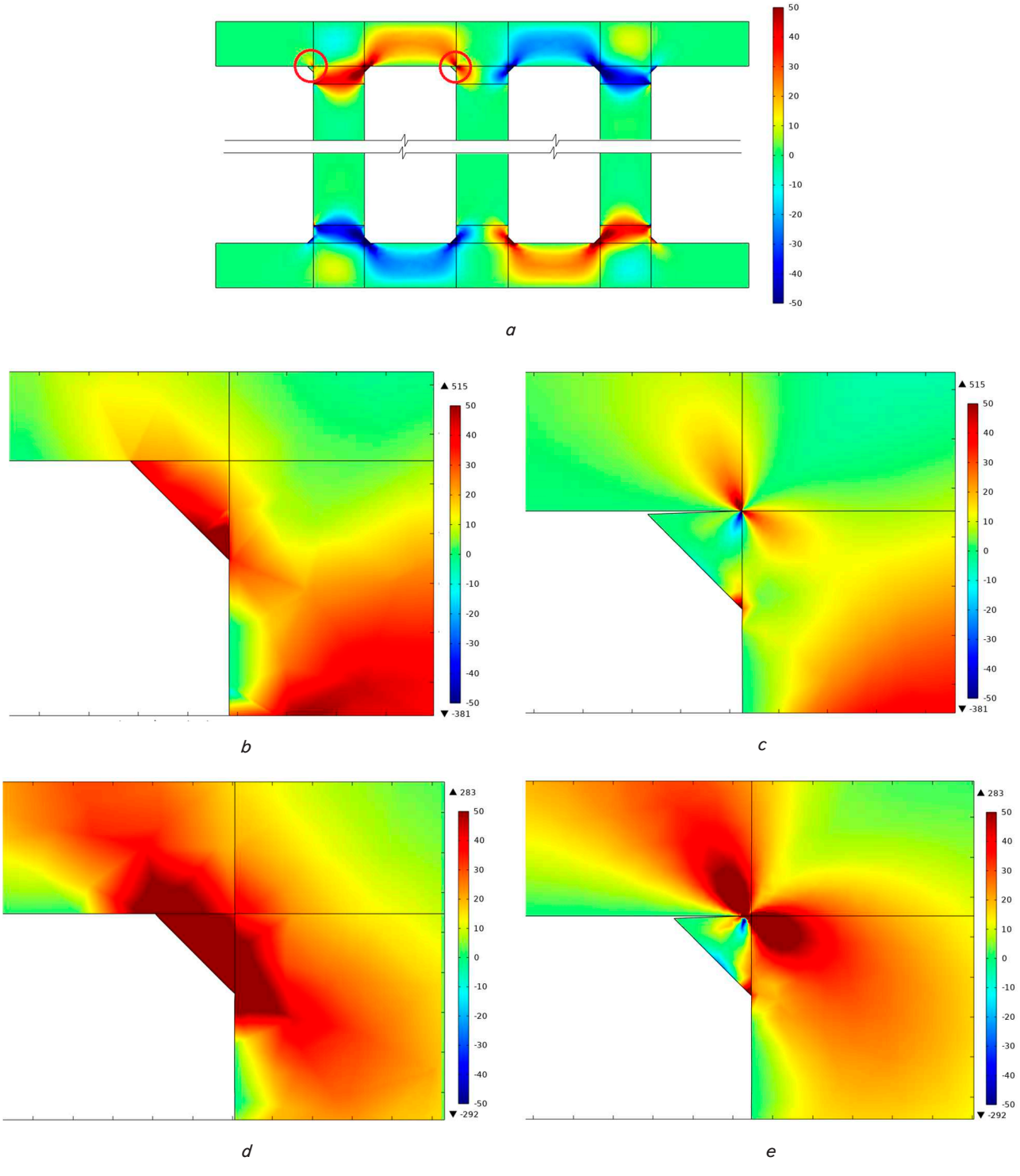

Fig. 2. Distributions of the tensor of mechanical stresses of the hydrogenerator when static eccentricity occurs (MPa):
a — in the plane of the central rod of the damper winding (circles show the areas of crack locations);
b — in the short-circuiting segment in the area of the solder joint of the extreme rod in the absence of a crack;
c — in the short-circuiting segment in the area of the solder joint of the extreme rod in the presence of a crack;
d — in the area of the solder joint of the central rod in the absence of a crack;
e — in the area of the solder joint of the central rod in the presence of a crack

5. 3. Modeling the emergence of a crack in the middle of the outer surface of the short-circuiting segment

A crack in the middle of the outer surface of the short-circuiting segment (mark 3 in Fig. 1, *c*) can form due to time-varying deformations since there are increased TMS values in this area. The destruction of the short-circuiting segment occurs not near the surface but primarily near the sharp edge of the crack in the thickness of the material itself.

Fig. 3, *a, b* shows the linear distribution of TMS value in the copper mass of the short-circuiting segment near the solder joint (shown by a bold red line) without a crack and in its presence.

Fig. 3, *c, d* shows the distribution of TMS value in the short-circuiting segment at depths of 0.05 mm (Fig. 3, *c*) and 2 mm (Fig. 3, *d*) below the surface along the entire length of the segment. The plot is for two options:

1) without a crack (curve 1 in Fig. 3, *c, d*);

2) with a crack (curve 2 in Fig. 3, *c, d*) on the outer side of the short-circuiting segment.

Fig. 3 demonstrates that when cracks appear, the values of TMSs increase exponentially and significantly depend on their location in the elements of the damper winding.

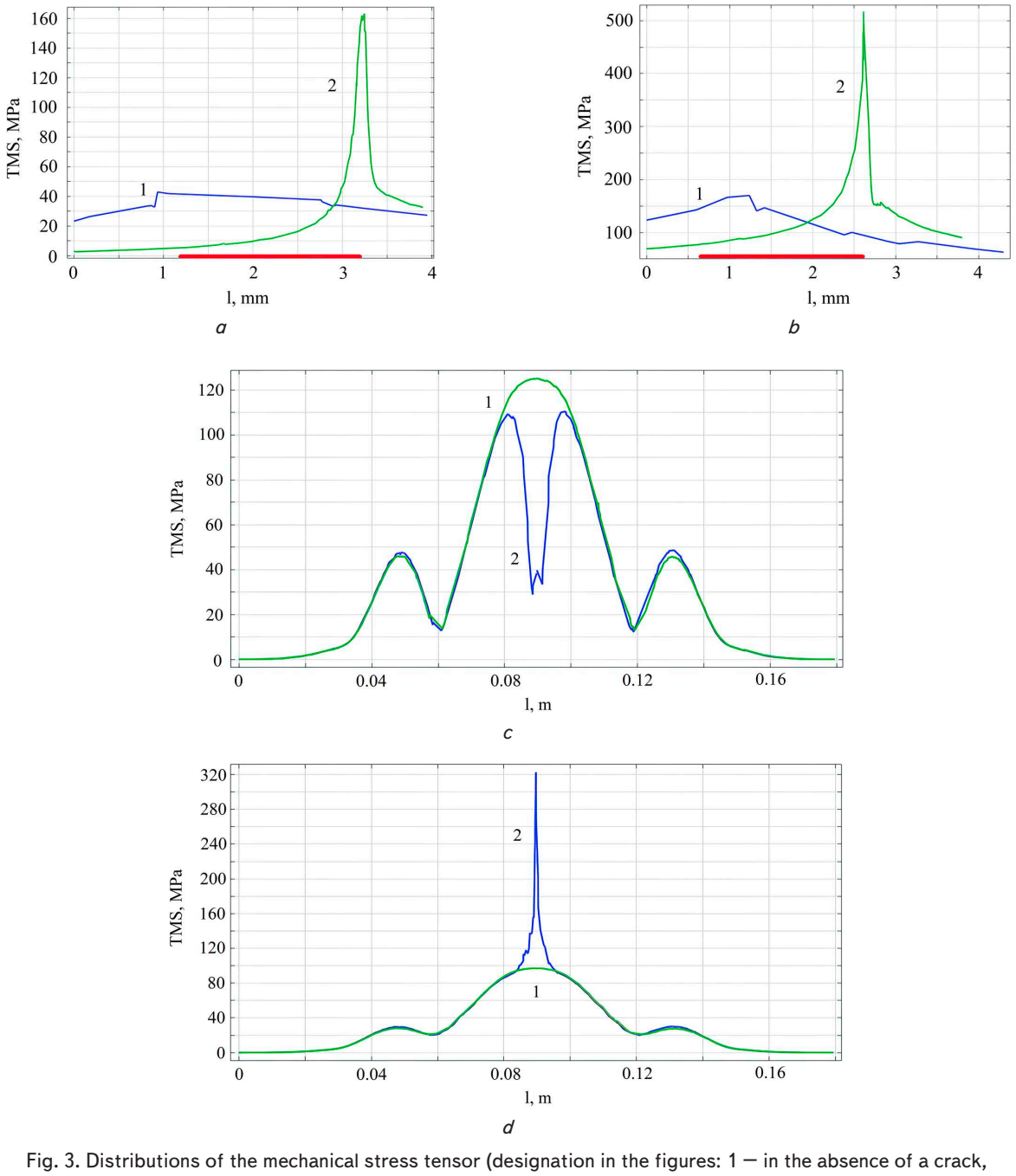

Fig. 3. Distributions of the mechanical stress tensor (designation in the figures: 1 – in the absence of a crack, 2 – in the presence of a crack): *a* – in the area of the short-circuiting segment in the area of the solder joint near the extreme rod; *b* – in the area of the short-circuiting segment in the area of the solder joint near the central rod; *c* – in the array of the short-circuiting segment at a depth of 0.05 mm below the surface; *d* – in the array of the short-circuiting segment at a depth of 2 mm below the surface

5. 4. Modeling the separation of the central rod of the damper winding

During the study, a simulation of the processes that will occur in DW when its central rod is separated was carried out. This type of damage can occur, including due to exceeding the TMS of the material's tensile strength when a crack appears at the point of attachment of the central rod to the short-circuiting segment (curve 2 in Fig. 3, *b*).

Fig. 4, *a* shows the radial bending of the outer side of the short-circuiting segment, which has a crack in the middle. The magnitudes of the deformations of DW are increased by 500 times for clarity. Fig. 4, *b* shows the axial bending of the short-circuiting segment of the two-rod model of the DW pole and the distribution of TMSs in the DW array when the central rod breaks. Fig. 4, *c* shows the distribution of TMS value in the material of the short-circuiting segment at a depth of 2 mm (under the surface on the outer side) along its entire length both when a crack appears on the outer side (curve 1 in Fig. 4, *c*) and when the central rod fails (curve 2 in Fig. 4, *c*).

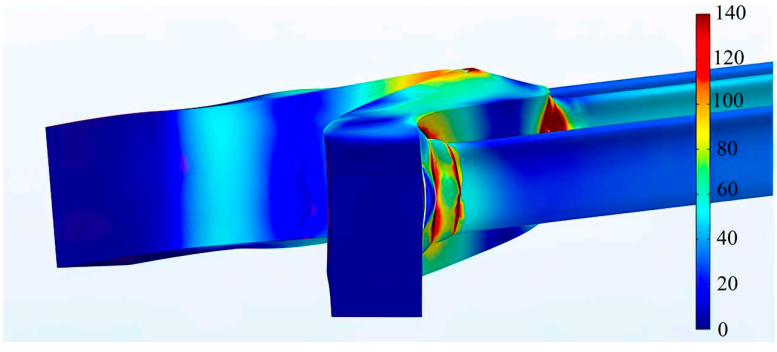

a

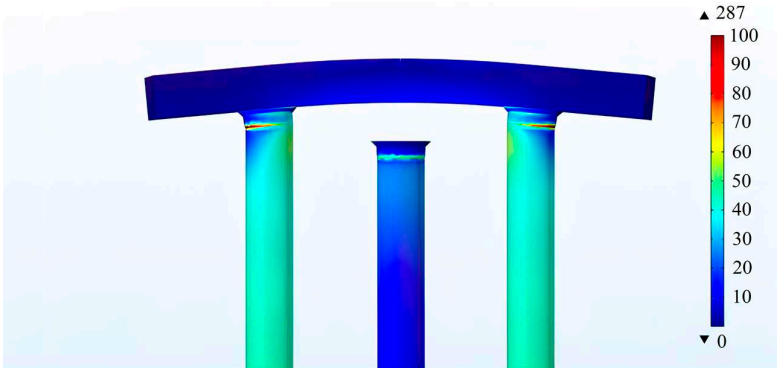

b

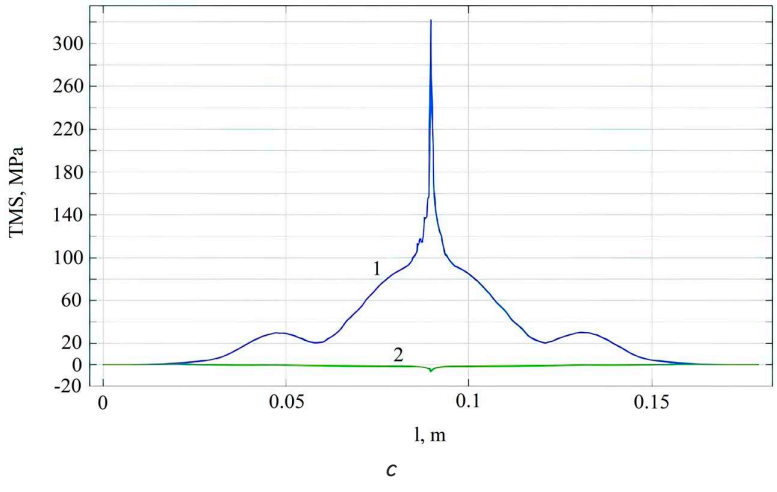

c

Fig. 4. Distributions of the mechanical stress tensor: *a* — three-dimensional, showing the radial bending of the short-circuit segment of the three-rod model of the damping winding, which has a crack in the middle on the outer side (the deformation values are increased by 500 times for clarity); *b* — three-dimensional, showing the axial bending of the short-circuit segment of the two-rod model of the damping winding of the pole, which has a crack after the separation of the central rod (the deformation values are increased by 200 times for clarity); *c* — in the material of the short-circuit segment at a depth of 2 mm below the surface on the outer side along its entire length (plot designations: 1 — when a crack appears (corresponds to option *a*), 2 — when the central rod is destroyed (corresponds to option *b*))

Fig. 4, *c* demonstrates that when transitioning from the "existing crack" state to the "break" state of the central rod, a huge difference in TMSs occurs in the middle of the short-circuited segment, which leads to its destruction.

5. 5. Modeling of free bending deformations of the short-circuit segment of the damper winding

The design of the hydrogenerator, which is considered in this study, does not provide for the possibility of axial displacement of the damper winding rods in the slots of the pole tip under the influence of various kinds of forces. This circumstance does not allow the rods of DW to occupy a position that corresponds to a certain level of thermomechanical deformations, and this, in turn, is actually an additional reason for the rods breaking off from the short-circuit segment (Fig. 1, *a*).

Fig. 5, *a*, *b* shows the bending deformations of the DW segment of one pole, which is under different conditions and states.

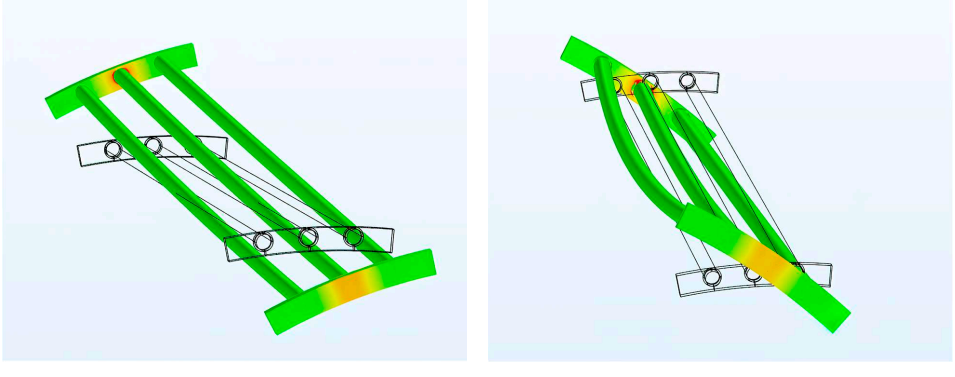

a *b*

Fig. 5. Bending deformations of the damper winding: *a* — without cracks with the possibility of free movement of the rods in the grooves (the deformation values are increased by 3 times for clarity); *b* — with the presence of cracks near the central and leftmost rods and with the possibility of their free movement in the grooves (the deformation values are increased by 25 times for clarity)

Analysis of Fig. 5, *a*, *b* reveals that the presence of cracks in the welds of DW against the background of the static eccentricity of HG rotor significantly distorts the shape of the bending deformations.

6. Results of research on the processes of crack formation and destruction of the rotor damper winding: discussion

To analyze crack formation in the damper winding, three local scenarios were considered: two rod seams and a crack in the middle of the outer surface of the short-circuiting segment. To assess the consequences of the complete separation of the central rod from the short-circuiting segment, an analysis of local thermomechanical stresses and deformations was performed. The latter damage may occur due to exceeding the local TMSs of the strength limit of the material of DW elements.

Fig. 1, *b* demonstrates that the central rod is the least heated: its temperature is close to the temperature of the pole core (~75°C), while the temperature of the extreme rods is significantly higher (~93.1°C). These results are consistent with the data reported in [7, 8], which show an increase in temperatures in the extreme rods with static eccentricity. As a result, the induced EMF excites current loops within the pole along the outer annular loop of the short-circuited fragment of DW, and the extreme rods carry a larger share of current/losses. The calculated values of the currents in the extreme rods are about 3,245 A (current density up to ~13.5 A/mm^2, which significantly exceeds the acceptable for transient regimes ~2.37 A/mm^2). Accordingly, the extreme rods undergo greater thermal elongations in the axial direction than the central one, which forms deformation gradients and local areas of increased TMSs in the seams and segment. Such a thermomechanical imbalance is the root cause of the genesis of cracks and bending deformations of DW arc segment.

The spatial maps of currents, temperatures, and TMSs obtained in our work are consistent with the generalized conclusions on the consequences of eccentricity and with diagnostic methods [1, 2]. In [3–5], the influence of regime factors, eccentricity and/or TMS without explicit defectology was analyzed. In comparison with them, the 3D coupled modeling proposed here clarifies the localization of TMS peaks precisely in the seams and in the middle of the segment and adds explicit modeling of cracks.

The increased temperature gradients in the zone of the extreme rods and the short-circuiting segment obtained in our work are consistent with the trends in the distribution of cooling flows and heat exchange given in [7, 8]. In contrast to the above works, we have performed coupled electromagnetic-thermal-mechanical modeling. It transfers the calculated temperature fields into thermal loads for the strength problem and makes it possible to directly estimate local TMSs in structural elements.

The asymmetry of currents and temperatures (increased values in the extreme rods) revealed in the study corresponds to the results reported in [9, 11, 12] regarding the role of tooth-and-groove effects and current-closing circuits in capsule hydrogenerators. The proposed approach brings this picture to the level of local strength criteria, demonstrating how electromagnetic and thermal asymmetries are transformed into TMS peaks and crack initiation in the seams and segment.

Work [10] shows that the results of the calculation of losses and heating significantly depend on the selected electromagnetic model (for example, taking into account/not taking into account the tooth-and-groove effects, spatial three-dimensionality, armature reaction). This model uncertainty can be transferred to thermal estimates and, ultimately, to estimates of thermomechanical stresses. In our study, coupled electromagnetic-thermal-mechanical modeling with a consistent transfer of calculated losses to thermal and strength statements was used, which reduces the accumulation of error due to the inconsistency of the models at different stages of the calculation. At the same time, operational observations of overheating and local burning (erosion) of the pole shoe surface [6] are consistent with the risk zones identified in the work in the short-circuit segment.

Unlike studies in which analysis was limited to the distributions of TMSs without explicit modeling of cracks

[3–5, 7–12], in our work three typical defects were parametrically modeled. Wedge-shaped cracks in the seams of the extreme and central rods and a crack in the middle of the outer surface of the short-circuiting segment were simulated. This approach makes it possible to trace the chain "inhomogeneous currents → uneven heating → local TMSs → localization/evolution of cracks → loss of segment integrity". That became possible due to the improvement of the three-dimensional model with coupled electromagnetic-thermal-mechanical analysis and explicit consideration of the geometry of cracks in critical zones.

As is known, TMSs can act both in tension and in compression. For crack initiation, local tension is decisive (areas 1, 2 in Fig. 1, *c*). The prolonged action of cyclic compression, exceeding the yield strength, causes residual deformations and, ultimately, can also lead to crack formation (area 3 in Fig. 1, *c*). Therefore, the assessment of only the stress state in the plane of the soldered joint is insufficient – an analysis of the zone around the joint is necessary, which after soldering functions as a single array with the joint and determines the real strength of the joint. Thus, our results confirm the critical role of tensile TMS cells in joints (in agreement with [3]) and supplement them with their localization on the joint geometry, which was lacking in previous publications.

Analysis of TMS distribution (Fig. 3, *a, b*) clearly shows that in the intact solder joint of the leftmost rod, the maximum TMS falls on the end of the joint and is ~41 MPa (blue curve). And in the presence of a crack – ~164 MPa (~ 4-fold increase, green curve). Similarly for the central rod: ~170 MPa without damage and ~540 MPa with a crack (~ 3.2-fold increase), while the maximum is shifted to the beginning of the joint – closer to the rod. The obtained value of 540 MPa exceeds the tensile strength of the copper of the joint/rod, which can lead to the separation of the central rod from the short-circuiting segment. Qualitatively, this corresponds to the mechanisms of degradation of nodes with weakened joints (see the generalization in [1]) and operational observations of local overheating/damage in capsule machines [6]. Similar local TMS peaks were previously identified in [3, 5], but in our study they are reproduced taking into account explicit crack modeling.

Thus, the triggering factor for the destruction of DW is local peaks of TMSs in the seams of the central and extreme rods. After the detachment of the central rod, the extreme rod becomes the next most vulnerable (Fig. 1, *a*); with a larger number of rods and similar conditions, an avalanche-like scenario of destruction is possible. In addition, in the event of a rod detachment on the opposite side of the pole, the deformation of the short-circuiting segment under the action of centrifugal forces can cause contact/damage to the frontal parts of the stator winding. This situation potentially leads to an emergency shutdown of HG. Similar secondary risks are consistent with practical conclusions regarding capsule structures [4, 7]. The behavior of TMSs in the thickness of the segment material is important. The plots in Fig. 3, *c, d* demonstrate that at a depth of ~0.05 mm under the surface of the segment, the emergence of a crack leads to a decrease in TMSs by approximately three times (curve 2 in Fig. 3, *c*). At a depth of ~2 mm, TMSs increase sharply (curve 2 in Fig. 3, *d*) to a level of 320 MPa. This value exceeds the yield strength of copper ($\sigma_{tk\_Cu} = 280$ MPa) and is 83% of its tensile strength ($\sigma_{mc\_Cu} = 390$ MPa). This indicates the formation of damage accumulation centers in the subsurface layers of the segment and progression to residual deformations/instability.

In addition to axial elongations, radial expansions and bends occur in the short-circuited segment zone. According to Fig. 4, *a*, the maximum curvature (bend) is recorded in the area of the central rod. This increases the load on the crack in the middle of the outer surface of the segment and is combined with the action of local TMSs in this area. At the moment of separation of the central rod, the instantaneous difference in TMSs in the middle of the segment reaches ~ 326 MPa, which contributes to the initiation or growth of a crack or even a sudden fracture of the segment in this zone. In this case, not only the magnitude but also the sign of the stresses changes (from compression to tension), which radically affects the stability of the defect. Taking into account the influence of geometric parameters on the fields/currents shown in [9, 11], the obtained asymmetric bending response is an expected consequence of the detected asymmetries.

The redistribution of forces after the separation of the central rod increases the risk of loss of integrity of the extreme rod. The reason is the emergence of a bending moment in the area of the exit of the extreme rod from the groove of the pole tip (leverage effect), where the calculated TMSs reach ~ 263 MPa. This is the situation that explains the observed (in Fig. 1, *a*) combined failure – damage to both the central and extreme rods. This is consistent with the conclusions from [12] regarding the asymmetry of eddy currents in the rods and its role in the occurrence of dangerous local stresses.

Having analyzed the results in chapter 5. 5, we can conclude that static eccentricity can cause not only the separation of the central rod but also the destruction of the short-circuiting segment itself. The key design risk factors are insufficient mobility of the rods in the pole piece slots and a small number of rods in the segment (oddity induces a "weak link"). These findings correlate with engineering recommendations for rotor optimization in capsule HGs [4, 7–9, 11].

The assessment of free bending deformations of DF (Fig. 5) demonstrates the role of geometric and defect asymmetry. For a conditionally "free" DF (without seams and defects), the bending is practically symmetrical, with a maximum deformation of up to ~40 mm (Fig. 5, *a*). In the presence of cracks in the seams of the extreme left and central rods, the bending becomes clearly asymmetric (Fig. 5, *b*), the maximum deformation decreases (~3.5 mm) but is concentrated near the defective side. This qualitatively confirms the role of cracks in the formation of the bending response. The shape of the deformations significantly depends on the type, size, and localization of the defects.

Comparison with the literature and contribution to solving the problem (chapter 2). Unlike studies in which electromagnetic and thermal aspects or 3D-TMS without explicit defectology were worked out in detail, our results bridge the noted gap. A coupled electromagnetic-thermal-mechanical analysis is provided up to the level of localization of TMS maxima in the seams and segment, the scenarios "crack → rod breakage → avalanche-like fracture of the segment" and the influence of cracks on the bending response are shown. This forms engineering-suitable risk criteria for assessing the durability/reliability of capsule hydrogenerators with an existing SE.

Based on our results, the following structural and technological measures have been proposed to reduce the risk of failures of pole DW:

1. Increasing the mobility of the rods in the grooves (for example, insertable insulated bushings with high-temperature lubricant).

2. An even number of rods in the segment.

3. Increasing the number of rods (smaller diameter of each).

4. Locally increasing the diameter of the extreme rods.

5. Considering the possibility of using materials of increased strength (brass/bronze) with an assessment of the compromise "strength ↔ losses".

These measures correlate with the identified failure mechanisms and could be integrated at the stages of modernization/repair.

Our study focuses on steady-state rated mode and static eccentricity; shock loads, short-term asynchronous modes, and cyclic temperature effects during frequent starts/stops were not taken into account. Further studies should be directed to expand the scenarios (dynamic eccentricity, transient and quasi-static modes), to analyze statistics of weld defects, and to experimentally validate subsurface TMS peaks.

7. Conclusions

1. A three-dimensional field model of coupled electromagnetic-thermal-mechanical analysis of the damper winding segment has been built, which makes it possible to determine 3D distributions of temperature, TMSs, and deformations in DW. The maximum temperature of the extreme rods in the model reaches ~93.1°C, and the current density is up to ~13.5 A/mm^2, which exceeds the permissible values for transient modes (~2.37 A/mm^2). Critical zones of potential crack formation have been identified, namely, the solder joints of the rods and the middle of the outer surface of the short-circuiting segment.

2. According to our simulation results, it was found that in the solder joint of the extreme left rod, the maximum of TMSs falls on the end of the joint and increases approximately 4 times in the presence of a crack. In the joint of the central rod, the maximum is shifted to the beginning of the joint (closer to the rod) and increases approximately 3.2 times to 540 MPa, which exceeds the tensile strength of copper. This value of TMS explains the probable separation of the central rod from the short-circuiting segment. Therefore, the initiation of DW fracture is determined by the local maxima of TMSs in the joints of the central and extreme rods.

3. For a crack in the middle of the outer surface of the short-circuiting segment, it was found that at a depth of ~ 0.05 mm below the surface, the TMS value is reduced. However, at a depth of ~ 2 mm, TMS increases sharply to a level exceeding the yield strength of copper. This leads to residual deformations and brings the segment closer to loss of integrity.

4. It is shown that static eccentricity can initiate a cascade failure scenario. The moment of separation of the central rod is accompanied by an instantaneous drop in TMSs in the middle of the segment (~326 MPa) and a change in the sign of stresses (from compression to tension), which contributes to the initiation/growth of a crack or rapid fracture of the segment in this zone. The redistribution of forces increases the risk of separation of the extreme rod (~263 MPa) due to the leverage effect at the exit from the groove.

5. It has been determined that the emergence and localization of cracks in the welds significantly change the bending (deformation) response of pole DW segment. Without defects, the bending is almost symmetrical, in the presence of cracks – asymmetric with a concentration of deformations on the defective side, which confirms the dominant influence of defects on the bending shape.

Conflicts of interest

The authors declare that they have no conflicts of interest in relation to the current study, including financial, personal, authorship, or any other, that could affect the study, as well as the results reported in this paper.

Funding

The study was conducted without financial support.

Data availability

All data are available, either in numerical or graphical form, in the main text of the manuscript.

Use of artificial intelligence

The authors used artificial intelligence technologies within acceptable limits to provide their own verified data, which is described in the research methodology section.

References

1. Mostafaei, M., Faiz, J. (2021). An overview of various faults detection methods in synchronous generators. IET Electric Power Applications, 15 (4), 391–404. https://doi.org/10.1049/elp2.12031
2. Ehya, H., Nysveen, A., Nilssen, R., Liu, Y. (2021). Static and dynamic eccentricity fault diagnosis of large salient pole synchronous generators by means of external magnetic field. IET Electric Power Applications, 15 (7), 890–902. https://doi.org/10.1049/elp2.12068
3. Vaskovsky, Yu. M., Geraskin, O. A. (2021). Influence of regime and operational factors on the damper system of the sali-ent-pole synchronous machine rotor. Tekhnichna Elektrodynamika, 2021 (2), 47–57. https://doi.org/10.15407/techned2021.02.047
4. Vaskovskii, Yu. M., Geraskin, O. A. (2020). The effect of rotor eccentricity on damper winding of 23 MVA capsular hydraulic-turbine generator. Hidroenerhetyka Ukrainy, 1-2, 59–64. Available at: https://uhe.gov.ua/sites/default/files/2020-07/15.pdf
5. Vaskovskii, Yu. M., Geraskin, O. A., Tatarinov, K. M. (2020). Simulation of thermomechanical stresses of the dampper winding of capsular hydrogenerator when the rotor eccentricity appears. Hidroenerhetyka Ukrainy, 3-4, 64–67. Available at: https://uhe.gov.ua/sites/default/files/2020-12/17.pdf

6. Zhou, Z.-T., Yang, Y., Xiao, K., Fan, Z.-N., Bian, Z.-Y., Wen, K. et al. (2020). Analysis and Treatment of an Overheated Ablated Fault on the Pole Shoe Surface of a Large Tubular Hydro-Generator. IEEE Access, 8, 127929–127938. https://doi.org/10.1109/access.2020.3008253
7. Zhang, S., Li, W., Li, J., Wang, L., Zhang, X. (2014). Research on Flow Rule and Thermal Dissipation Between the Rotor Poles of a Fully Air-cooled Hydro-generator. IEEE Transactions on Industrial Electronics, 62 (6), 3430–3437. https://doi.org/10.1109/tie.2014.2366723
8. Jichao, H., Yufei, L., Jiechen, D., Yutian, S., Baojun, G., Weili, L. (2021). Thermal Modeling and Experimental Validation in the Rotor Region of Hydrogenerator With Different Rotor Structures. IEEE Access, 9, 120001–120009. https://doi.org/10.1109/access.2021.3098319
9. Fan, Z., Liao, Y., Han, L., Xie, L. (2013). No-Load Voltage Waveform Optimization and Damper Bars Heat Reduction of Tubular Hydrogenerator by Different Degree of Adjusting Damper Bar Pitch and Skewing Stator Slot. IEEE Transactions on Energy Conversion, 28 (3), 461–469. https://doi.org/10.1109/tec.2013.2259628
10. Xu, M., Hu, W., Zhou, Z., Fan, Z. (2024). The influence of electromagnetic field models on the damper winding loss and heat calculation results of tubular hydro-generator. Electronics Letters, 60 (5). https://doi.org/10.1049/ell2.13144
11. Bian, Z., Zhou, Z., Fan, Z. (2021). No-load voltage and damper winding loss and heat analysis of the pole shoe and damper winding centre line shifted structure of tubular hydro-generators. Electronics Letters, 57 (18), 691–693. https://doi.org/10.1049/ell2.12227
12. Qiu, H., Fan, X., Yi, R., Feng, J., Wu, J., Yang, C., Zhao, H. (2017). Eddy current density asymmetric distribution of damper bars in bulb tubular turbine generator. Archives of Electrical Engineering, 66 (3), 571–581. https://doi.org/10.1515/aee-2017-0043